Solid Freeform Fabrication 2023: Proceedings of the 34th Annual International Solid Freeform Fabrication Symposium – An Additive Manufacturing Conference
Reviewed Paper

ADDITIVE MANUFACTURING OF PERSON SPECIFIC DIABETIC FOOT INSOLES WITH ADJUSTABLE CUSHIONING PROPERTIES USING TPMS LATTICE STRUCTURES

F. R. Claybrook*, D. J. Southee*, and M. I. Mohammed*

*School of Design and Creative Arts. Loughborough University, Loughborough, LE11 3TU

Abstract

Complications associated with diabetes are numerous, including foot problems which in extreme cases can lead to amputations. Current management involves the use of foam diabetic foot insoles (DFI) to provide cushioning, however load bearing capacity is limited, and designs often do not provide a comfortable or efficacious fit. This study aspires to resolve problems using digital fabrication workflows. The exploration of potential 3D scanning of anatomical data, parametric modelling, and additive manufacturing was created for a patient specific DFI. This demonstrated that patient scanning data provides means to create a custom fitting insole template, improving overall fit. Demonstrating the use of triply periodic minimal surface (TPMS) structures, fabricated in Thermoplastic Polyurethane (TPU), as cushioning structures, whereby unique lattice designs allow regionally tailored mechanical loading properties of the insole concept. The final insole realises a superior alternative to tradition DFI.

1. Introduction

The complexity of anatomical representation of the body is one that has been researched to improve clinical processing and burdens on healthcare providers (Mohammed et al., 2016). Diabetic patients increase complications in orthotics with the presence of Peripheral Neuropathy. Current diabetic insoles are established by the International Working Group on Diabetic Foot 2015 guidelines dictating the requirement of custom-made therapeutic footwear to relieve pressure <30% and the importance of preventive techniques, though the research is sparse (Bus et al., 2015). The current rehabilitation techniques involve patients to daily self-examine and wear properly fitting footwear (Schaper, et al 2016). Yet these intervention techniques are perturbed by cost, time, dexterity, and health impairments, resulting in low conformity with upkeep (Salles & Gyi, 2013; Van Netten et al., 2013).

Prosthetic based rehabilitation techniques using insoles requires laborious and intensive production process. The methodology is costly with a dedicated infrastructure for negative impressions, plaster infill, and vacuum formation for therapeutic footwear (Farhan et al., 2021), limiting manufacturing to highly skilled professionals (Davia-Aracil et al., 2018). The plaster is reusable with the breakdown of the substance for repetitive use, but this destruction of the mould means the anatomical data of a patient is not kept for repeat prescriptions and can increase wait times. The workflow of traditional fabrication techniques has been summarised by Mohammed et al., 2018. The complex process of plaster cast can be defective in the fitting and sculpting process and forming can cause discomfort; even consequential movements from the patients can differ the accuracy of this application process. Too much variability in successful casting makes the process too dependent on the rectification process, indicating a better need for a clinical workflow (Farhan et al., 2021).

The recent development of computer aided design (CAD) allows the advancement of 3D replicated scanning and manufacturing to have a higher customisation level than foams on the market by customising to microporous architecture (Mohammed & Gibson, 2018; Sala et al., 2022). Foot scans can be based on geometric point clouds to retrieve the best developed fit (Rout et al., 2010) whilst keeping a non-invasive approach to be easily adopted into clinical practice. Current overlapping technologies involve gypsum plaster and 3D scanning; gypsums white matte appearance is ideal and creates and an excellent skin replication (Paterson, 2013). The use of a replicated limb allows more leverage for scanning, lowering obstruction and mobility to capture anatomical data. With scanning technologies becoming cheaper and more accessible to the public (Haleem & Javaid, 2019), the medical application of this technology can potentially be complementary to the field. Research can take advantage of exploring a full augmentation for a complete digital fabrication process without the need for physical casting. An adaptation of Paterson, 2013 for digital orthoses application for gypsum casting has been adapted for full augmentation in Figure 1. This will be explored for the study.

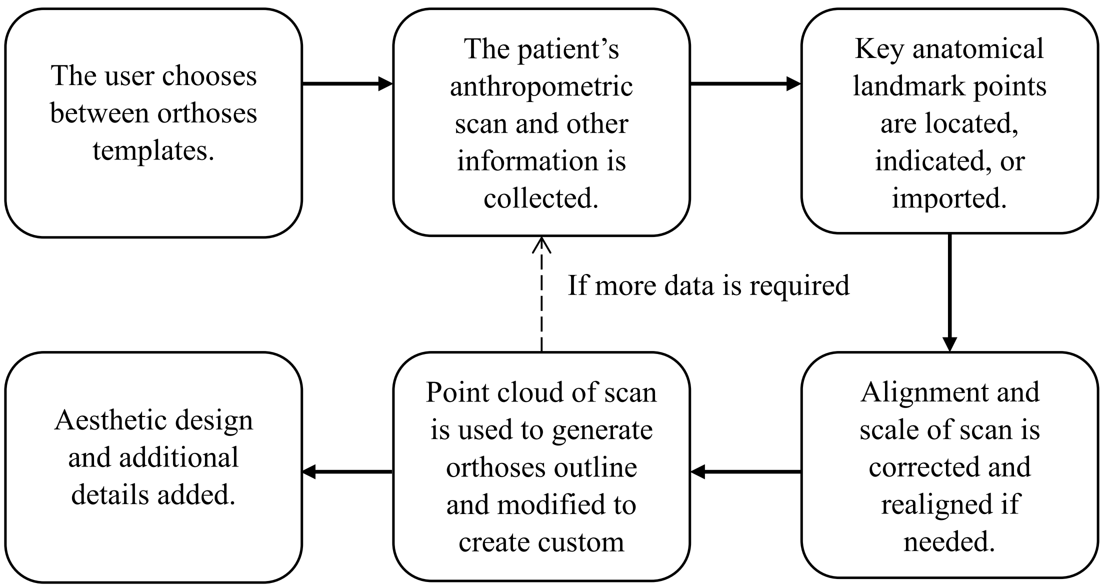

Figure 1 - Adaptation of Paterson, 2013 3D CAD flow for 3D scanning orthoses application

The use of fuse fabrication filament (FFF) modelling allows improved technologies and the use of lower shore hardness and malleable materials, such as Thermoplastic Polyurethane (TPU) (Harris et al., 2019). The small, compact, and sterile environment created by FFF is favourable to the medical sector, providing a quicker and higher customisable option of manufacturing. Traditional manufacturing is limited by tooling, whereas additive manufacturing (AM) is advantageous as it is tool free manufacturing and can reproduce high levels of complexity, such as lattice structures, ideal for tailored specific energy absorption (Bates, *et al.,* 2016; Claybrook, *et al.,* 2022). The high elasticities and energy absorptions characterised by TPU creates a polymer suitable for applications to control mechanical deformations (Beloshenko et al., 2021). The use of TPU lattices can further cushioning applications, alongside 3D scanning creating a heavily customised insole approach, both mechanically and physically.

Lattice structures provide a high strength-to-weight ratio but there has been limited research with triply periodic minimal surface (TPMS) structures (Beloshenko et al., 2021). The development of the TPMS network and control of porosity can lead to high level customisation that are attractive to the orthotic field. The complex geometry of TPMS structures creates a porous structural unit capable of the customisation needed for diabetic insoles (Ma et al., 2019). TPMS structure, TPU, and FFF are currently limited in studies (Claybrook et al., 2022; Holmes et al., 2022; Sala et al., 2022) and shows an opportunity in this field.

In this study we aim to investigate the limited guidelines for orthoses scanning techniques. Our techniques will propose less material waste, time, and labour than required for the traditional insole application techniques. The main objective is to understand the capabilities of the 3D scanning and the digitised process to accurately mimic the plantar surface foot for highly accurate custom-made insole. A specification will be developed for the requirements of a successful 3D scan for orthotic application, similarly the preliminary testing of an initial TPMS structure at insole height to understand the mechanical properties achievable.

2. Experimental Methodology

2.1. Topography Scanning Mapping

We initially assess the capabilities of professional 3D scanners, the Artec Leo, to identify limitations and boundaries of 3D scanning techniques. There is no widespread common practice for foot 3D scanning foot orthoses, therefore reported evidence from literature indicating high reliability of anatomical capturing foot data was followed (Mohammed & Elmo, 2020). To the authors knowledge, there is only one systematic review comparing reliability and accuracy of 3D scanning with traditional techniques for therapeutic footwear. Farhan et al., 2021 reported there was no evidence for accurate fabrication of foot orthoses, traditionally or contemporary, and requires future research. Though these practices were indicated for good reliability: Relaxed standing or sitting and partial weight bearing to accurately capture the forefoot and rearfoot width.

To model the practicalities of scanning a human foot, a prosthetic lower limb (PLL) was placed on a chair to mimic that of a patient with the foot partially raised. The fat pad expansion and weight could not be replicated at this stage but was considered for further development. The anatomical representation of the foot was collected using a PLL with a white matte finish. The Artec Leo (Artec 3D, Luxembourg) 3D scanning light reflectance technology created a digital imaging with 3D point accuracy up to 0.1mm and 3D resolution up to 0.2mm at 80 frames per second. The Artec Studio 16 software compiled the point cloud data and created a mesh from the scanned anatomical data. The software allowed for various further post processing stages to create a watertight model.

2.2. Parametric insole modelling

The model created in Artec Leo Studio 16 was then exported to Autodesk Fusion 360 (2.0.16265) for further development and construction of the plantar surface. The scanned model informed the development of the insole using a segmented plane through surface and solid modelling for the exportation into nTopology (3.41.2) for the corresponding TPMS to be inputted for the insole design. The approach offers sophisticated biomimicry and accurate plantar surface replication which was then assessed to evaluate the potential CAD-informed mechanical and pressure data.

2.3.Material and Methods

2.3.1. Gyroid Design and Manufacture

To understand the mechanical behaviour of TPMS structures at insole height for the appropriate lattice design, Gyroid, was chosen to demonstrate our proposed methodology. The upper and lower extremity of the insole were chosen at 10mm height and 5mm height from the approximations gathered from academic research (Ahmed et al., 2020; Bus et al., 2004; Guldemond et al., 2007). Previous research from Claybrook, *et* al., 2022; Holmes *et al.*, 2022, characterised TPU and TPMS structure with 10mm cell sizes following ASTM D695-15 standard for polymer compression (ASTM International, 2023), this approach was also used in this study. The cells can be examined in a full unit cell and half unit cell; 10mm and 5mm. Characterising test samples as 10mm height and 10mm cell (10CH), 10mm height and 5mm cell (10C5H) and 5mm height and 5mm cell (5CH). The strut thickness 1.2mm and 15mm diameter were used as a preliminary pilot for the capabilities of the structure at the different insole heights. The corresponding porosities are shown in Figure 2.

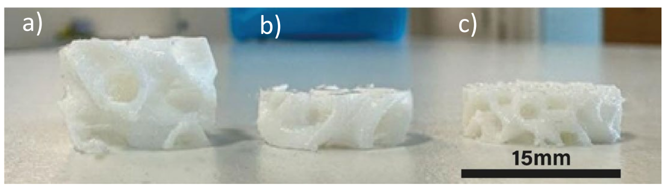

d)

Gyroid Strut Thickness (mm)	10mm Height 10mm Cell (%)	5mm Height 10mm Cell (%)	5mm Height 5mm Cell (%)
1.2	76.69	76.67	52.94

Figure 2- Gyroid porosities printed with 1.2mm strut thickness with a) 10mm Height, 10mm Cell, b) 5mm height and 10mm Cell, and c) 5mm Height and 5mm cell. d) a table representing the corresponding porosities with chosen strut thickness, height, and cell size.

Structures were fabricated using a Prusa i3 MK3S+ (Prusa Research, Czech Republic) FFF printer, using a shore hardness 90A TPU polymer (Technology Outlet, UK). The Gyroid structures were designed using nTopology to create STL files, prepared for slicing using the ‘generic flex’ profile within Prusa Slicer. The structures consisted of 0.2mm layer thickness, print speed 40mm/s, travel speed 60mm/s, nozzle size 0.4mm, 240ºC nozzle temperature and 50ºC bed temperature.

2.3.2. Mechanical Testing

Compression testing was conducted in accordance with ASTM D695-15 standard, except the 2:1 ratio guideline, to understand Gyroid behaviour at insole height. Tests were conducted on a 3366 universal test rig mounted with a 10kN load cell (Instron, UK). Samples were tested using an adjusted protocol described previously by Claybrook et al, 2022, where samples were maintained at 15mm diameter and two different heights of 10mm and 5mm. The test comprised of 7 repetitions of samples at a 1.2mm strut thickness compressed at a 1mm/min strain rate.

3. Results and Discussion

3.1. Scanning capabilities

The investigation in this study is to understand the ability of the Artec Leo in 3D capturing the anatomy for diabetic patient's feet to create appropriate prosthetics from patient specific data. The process of rotating around the patient leg, whilst in the seated position, demonstrated the need for the foot to be raised from the floor. In Figure 3a the distance between the scanner and the plantar surface of the foot created limitations in dexterity with the Artec Leo and a nature of invasive boundaries. The digitised PLL (Figure 3b) highlights the compromise of the point cloud topography at the back of the calf and heel of the foot. The heel is vital in insole manufacturing and requires accurate anatomical representation. Thus, a minimum distance of 40cm from the ground needs to be specified to increase accuracy and complete 360-degree capture of the foot.

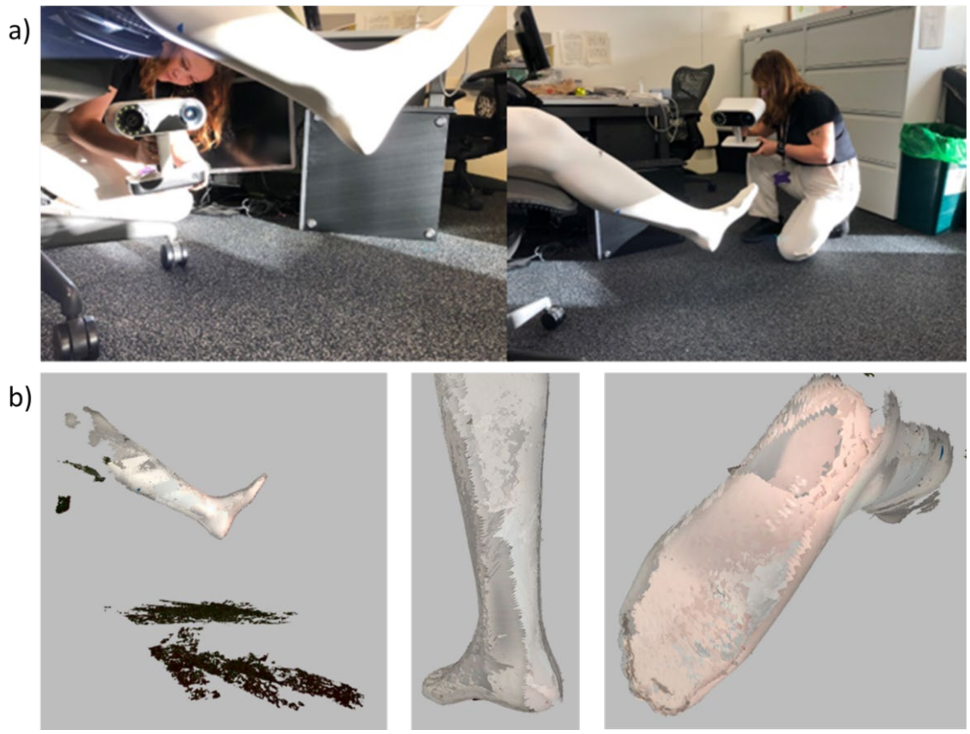

Figure 3 - a) Artec Leo scanning Prosthetic Lower Limb, b) Raw scanning image from Artec Leo Scans and imported into Artec Studio 16.

The expectation of a patient to hold their leg in a fixed partially raised position is near-impossible, raising practicality concerns and uncontrollable micro movements. Similarly, given the need for fat pad expansion, further apparatus is required to counteract involuntary movements and create a platform for the foot to be partially weighted. Salles & Gyi, 2013 created a raised platform with a scanner contained in a box with a clear cut out for the foot to be captured. As we want to create partially weighted instead of full weight distribution (Farhan et al., 2021), the use of a Perspex platform to withstand the force and create a clear image of fat pad expansion can be replicated for the use of handheld 3D scanning.

Another consideration is the use of the PLL is a matte white surface. This is captured excellently with the light surface for the scanner, this may cause complications with different skin pigmentation and requires further evaluation in future work. A possible solution to adjust for this consideration is to note key anatomical landmarks and record the length of the foot alongside the scan, to maintain scale. Therefore, the following specification is needed for handheld 3D scanning applications of the foot is seen in Figure 4.

Figure 4- Guidelines to consider for 3D scanning applications for anatomically representing the foot.

3.2. Model Fabrication

Scanning with the Artec Leo was used to inform the digital workflow of a heightened custom-made insole approach. The import of the PLL data into the Artec Studio software is shown in

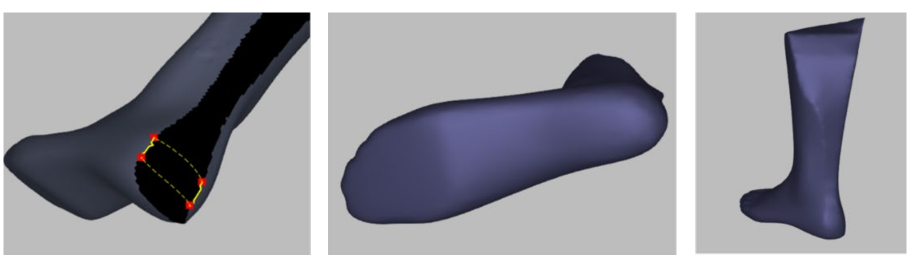

Figure 5- The fill holes option on Artec Studio 16. The use of manual bridging for increased control and accuracy.

Figure 3b. The software's ribbon was followed to understand the capabilities of the filling of data, holes and smoothing of the model while maintaining accurate anatomy.

The model produced with the superior design quality was achieved by bridging (Figure 5). This provided more control, following the natural curves of the PLL. With respect to intricate detailing such as toes, the scan managed to capture the grooves and surface texture when maintained in sharp fusion but lost some quality with the use of fast fusion. This is not of concern as the plantar surface is only of interest for insole manufacture, therefore fast fusion was optimal for a smoother surface to work with. The general anatomy was maintained with respect to overall characteristics and silhouette, such as arch height, but further research is needed for the effects on real life patients skin textures.

When the initial 3D model was imported, a plane was created below the plantar surface. This was then divided into multiple rectangular subdivisions to create vertices that can adapt to all the different curves of the plantar surface. The result of the pull to the surface of the Artec Leo scan resulted in a need to offset from the plantar surface (Figure 6a). Figure 6b demonstrates the rippling and self-inversion that resulted around the organic form of the foot, to avoid this the edges of the insole required smoothing for a cleaner parametric model (Figure 6c).

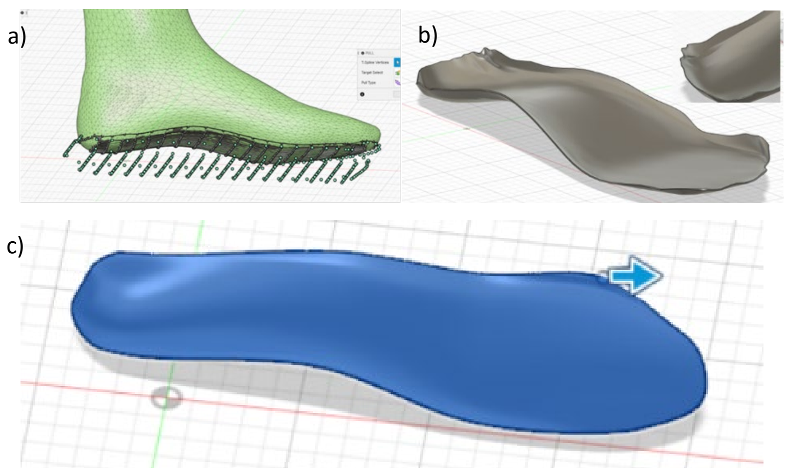

Figure 6 - a) snapping feature of plane to surface in Autodesk Fusion 360, b) Form of the insole surface model after thickening to insole height (5mm), and c) Insole smoothed to solid body for a simple offset of the prosthetic lower limb.

The modelled insole was exported to nTopology for tailored unique loading characteristics. Gyroid was chosen for a theoretical concept of the Smart Insole in Figure 7. This showcases the concept of the 'smart insole' split into the four main anatomical regions; toes, metatarasal heads, arch, and heel. Manufacturing is achieveable from a complete digitised process and customisation, including the corresponding required Gyroid and its mechanical properties. Patient specific peak pressure information would need to be acquired to inform this manufacturing, creating the opportunity to fully customise the insole from the digitising of the patients specific anatomy and corresponding peak pressure regions on the plantar surface for the appropriate Gyroid and its mechanical properties by functional grading of the insole.

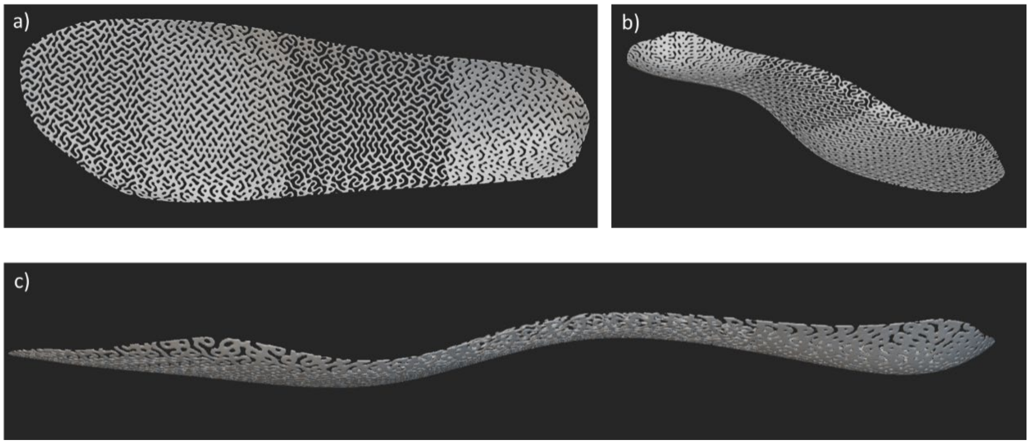

Figure 7 - Custom made insole from Artec Leo prosthetic lower limb scan data creating a smart insole concept controlled by regional compressive properties of the Gyroid structure a) front profile, b) isometric profile and c) side profile.

3.3. Cushioning Properties

Elastomeric structures complex deformable nature inhabits an undefined yield point as a clear break or permanent deformation is absent (Claybrook, *et al.,* 2022). The geometric configuration of Gyroid allows restoration of the scaffold with a prolonged elastic plateau for energy absorption. The designed porosity controls the characteristics of the Gyroid until complete densification, characterising the structure like solid TPU. Figure 8 shows a closer examination of the singular compression cycle for 10CH, 10C5H, 5CH. Buckling was absent across all porosities and cell sizes, creating a uniform collapse and lower unpredictability of the intrinsic structure. Furthermore, the validation of load axial column theory that buckling is eliminated in the less slender column structures.

Figure 8a shows the compressive modulus of the tested samples, with 5CH having the highest flexibility and 10CH the lowest. The intrinsic properties of the cell size and wall thicknesses indicate the importance of their designed volume of space. Even though the porosity of the 5CH is lower and more material deposited, the influence of the TPMS on the flexibility of the structure is more apparent.

The compression testing of the samples (Figure 8b, c, d, e) showed a high repeatability with minimal standard deviation. In comparison to Claybrook et al., 2022 Split P samples, the Split P approximation of pressure at 10% strain was 0.2-0.3MPa which is exhibited in 10CH and 10C5H (Table 1). In Figure 8, 5CH demonstrated a lower threshold that then exceeded both structures at higher strain rates of the samples. This suggests the porosity of the volume of space has a heavy influence on the initial collapse of the Gyroid structure, which is then controlled by the designed cell size. As each sample had the exact same strut thickness but due to their volume of space occupied possessed different porosities (Figure 2). In Figure 8b it shows there is no clear plastic plateau with 5CH unlike the others, proposing the designed porosity was removed from the structure quicker and densification is unclear in this malleable design, hence the higher MPa values >20% strain for 5CH. In Figure 8c, d, and e 10CH has the least variation in the repeated samples throughout the compression test, and 5CH the most; this could be due to the smaller detailed 5CH reaching the resolution of the FFF. Similarly, 5CH requires the highest load and 10CH the lowest with the tested 1.2mm sturt thickness.

To understand the energy plateau for each strut thickness, Table 1 shows 10CH, 10C5H, and 5CH up to 60% strain to identify the MPa capable. From this preliminary strut thickness, it can be assumed that 10mm height insole is preferable to 5mm height as it has a wider range of MPa covering DFUS. In future work we hope to examine Gyroid structures over a wider porosities and strut thickness for a more complete mechanical understanding.

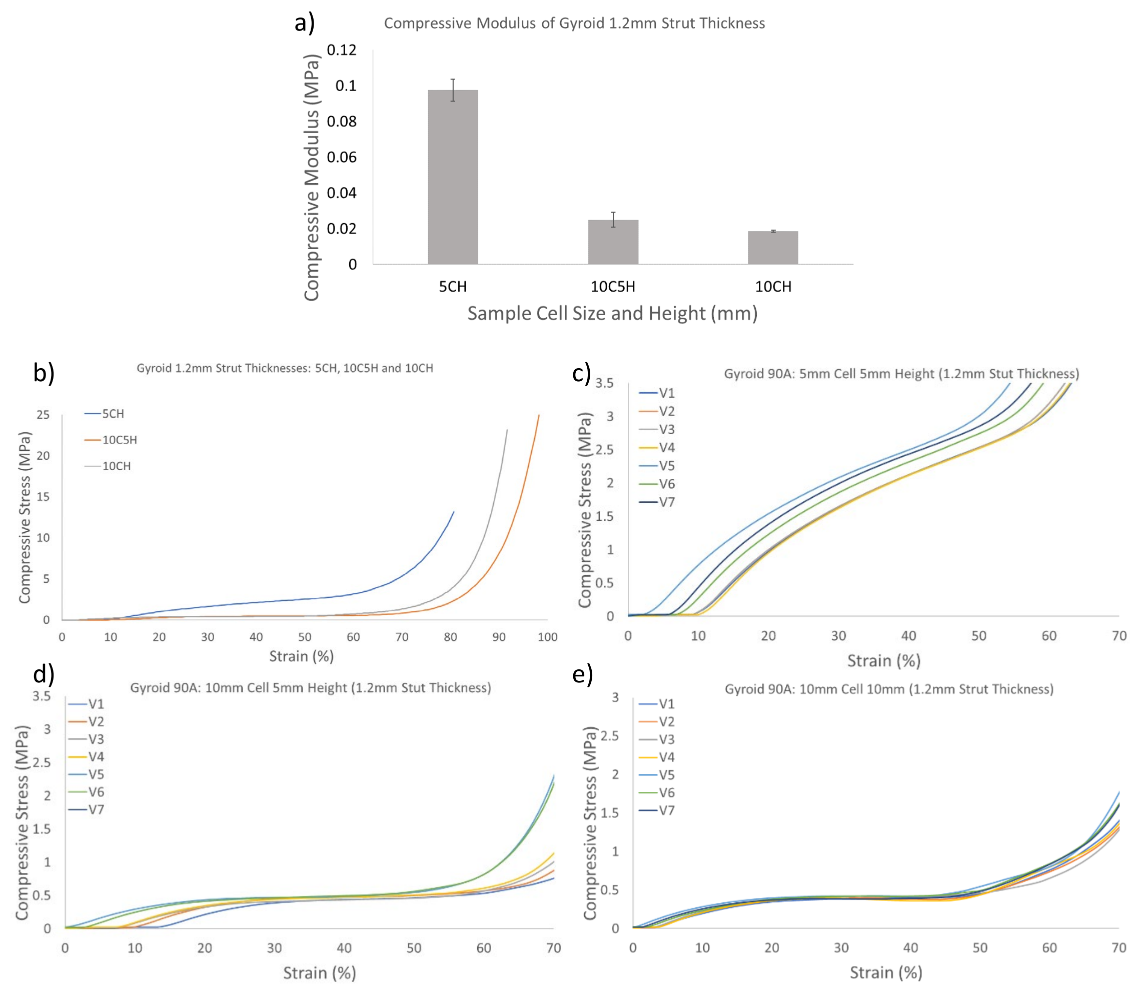

Figure 8 - Data from compressive loading of Gyroid 90A shore hardness TPU for 5CH, 10C5H, and 10CH. a) comparison of the compressive modulus of 1.2mm strut thickness, b) comparison of the average 5CH, 10C5H and 10CH stress strain profiles. The stress strain profiles of c) 5mm cell and 5mm height, d) 10mm cell and 5mm height, and e) 10mm cell and 10mm height.

Table 1 - Summary of the compressive modulus and compressive stress for all tested samples of 90A TPU Gyroid structures at upper and lower insole heights for 1.2mm strut thickness.

Shore Hardness 90A				Compressive Stress @ x Strain (MPa)					
Gyroid	Strut Thickness (mm)	Compressive Modulus (CM) (kPa)	CM Standard Deviation (kPa)	10%	20%	30%	40%	50%	60%
10mm Height, 10mm Cell	1.2 (76.7)	18.66	0.61	0.21	0.36	0.40	0.41	0.46	0.74
5mm Height, 10mm Cell	1.2 (76.7)	25.02	4.11	0.03	0.27	0.42	0.46	0.48	0.56
5mm Height, 5mm Cell	1.2 (52.9)	97.00	6.19	0.11	0.99	1.65	2.15	2.54	3.24

4. Conclusion

The work discussed has put a detailed characterisation to the workflow of applicable scanning technology needed for customised insoles. There is a potential of a complete digitised approach to the medical application of insole fabrication, which could replace the current labour intensive and qualitative techniques utilised clinically. The 3D scanning process has shown a high replication of anatomical landmarks of the feet and the suitability of mimicking the plantar surfaces and applying further 3D printing techniques.

The use of TPU and Gyroid structures has shown a possible alternative for insole manufacture with the upper and lower insole heights for characterisation in this study. The preliminary data collected has only used one strut thickness but showcases the possible use of Gyroid at 5mm and 10mm height for an alternative to foam. There is a wider range of geometrical configurations, TPMS, cell size, and porosity to be explored and attained through compression testing to fully understand this new approach to medical grade insole manufacturing. Similarly, the adjustment of the TPMS' in conjunction with the plantar anatomy to define the insole is in early stages. The curvature of the patient anatomy may create the need for support and will need to be explored further to limit this.

References

Ahmed, S., Barwick, A., Butterworth, P., & Nancarrow, S. (2020). Footwear and insole design features that reduce neuropathic plantar forefoot ulcer risk in people with diabetes: A systematic literature review. *Journal of Foot and Ankle Research*, *13*(1), 1–13. https://doi.org/10.1186/s13047-020-00400-4

Bates, S. R. G., Farrow, I. R., & Trask, R. S. (2016). 3D printed polyurethane honeycombs for repeated tailored energy absorption. *Materials and Design*, *112*, 172–183. https://doi.org/10.1016/j.matdes.2016.08.062

Beloshenko, V., Beygelzimer, Y., Chishko, V., Savchenko, B., Sova, N., Verbylo, D., Voznyak, A., & Vozniak, I. (2021). Mechanical Properties of Flexible TPU-Based 3D Printed Lattice Structures: Role of Lattice Cut Direction and Architecture. *Polymers*, *13*(17), 2986. https://doi.org/10.3390/polym13172986

Bus, S. A., Armstrong, D. G., van Deursen, R. W., LEWIS, J., Caravaggi, C. F., & Cavanagh, P. R. (2015). IWGDF Guidance on footwear and offloading interventions to prevent and heal foot ulcers in patients with diabetes. *© 2015 International Working Group on the Diabetic Foot*. https://doi.org/10.4324/9781315264820-10

Bus, S. A., Ulbrecht, J. S., & Cavanagh, P. R. (2004). Pressure relief and load redistribution by custom-made insoles in diabetic patients with neuropathy and foot deformity. *Clinical Biomechanics*, *19*(6), 629–638. https://doi.org/10.1016/j.clinbiomech.2004.02.010

Claybrook, F. R., Mohammed, M., & Southee, D. J. (2022). *Investigation of additive manufactured Split P TPMS elastomeric structures for diabetic foot insoles*. *4*(1), 1–4. https://doi.org/10.18416/AMMM.2022.2209664

Davia-Aracil, M., Hinojo-Pérez, J. J., Jimeno-Morenilla, A., & Mora-Mora, H. (2018). 3D printing of functional anatomical insoles. *Computers in Industry*, *95*, 38–53. https://doi.org/10.1016/j.compind.2017.12.001

Farhan, M., Wang, J. Z., Bray, P., Burns, J., & Cheng, T. L. (2021). Comparison of 3D scanning versus traditional methods of capturing foot and ankle morphology for the fabrication of orthoses: a systematic review. In *Journal of Foot and Ankle Research* (Vol. 14, Issue 1). BioMed Central Ltd. https://doi.org/10.1186/s13047-020-00442-8

Guldemond, N. A., Leffers, P., Schaper, N. C., Sanders, A. P., Nieman, F., Willems, P., & Walenkamp, G. H. I. M. (2007). The effects of insole configurations on forefoot plantar pressure and walking convenience in diabetic patients with neuropathic feet. *Clinical Biomechanics*, *22*(1), 81–87. https://doi.org/10.1016/j.clinbiomech.2006.08.004

Haleem, A., & Javaid, M. (2019). 3D scanning applications in medical field: A literature-based review. *Clinical Epidemiology and Global Health*, *7*(2), 199–210. https://doi.org/10.1016/j.cegh.2018.05.006

Harris, C. G., Jursik, N. J. S., Rochefort, W. E., & Walker, T. W. (2019). Additive Manufacturing With Soft TPU – Adhesion Strength in Multimaterial Flexible Joints. *Frontiers in Mechanical Engineering*, *5*. https://doi.org/10.3389/fmech.2019.00037

Holmes, D. W., Singh, D., Lamont, R., Daley, R., Forrestal, D. P., Slattery, P., Pickering, E., Paxton, N. C., Powell, S. K., & Woodruff, M. A. (2022). Mechanical behaviour of flexible 3D printed gyroid structures as a tuneable replacement for soft padding foam.

Additive Manufacturing, *50*. https://doi.org/10.1016/j.addma.2021.102555

Ma, Z., Lin, J., Xu, X., Ma, Z., Tang, L., Sun, C., Li, D., Liu, C., Zhong, Y., & Wang, L. (2019). design and 3d printing of adjustable modulus porous structures for customized diabetic foot insoles. *International Journal of Lightweight Materials and Manufacture*, *2*(1), 57–63.

Mohammed, M. I., Cadd, B., Peart, G., & Gibson, I. (2018). Augmented patient-specific facial prosthesis production using medical imaging modelling and 3D printing technologies for improved patient outcomes. *Virtual and Physical Prototyping*, *13*(3), 164–176. https://doi.org/10.1080/17452759.2018.1446122

Mohammed, M. I., & Elmo, F. (2020). *Digital design and fabrication of controlled porosity , personalized lower limb AFO splints*. *2*(1). https://doi.org/10.18416/AMMM.2020.2009013

Mohammed, M. I., Fitzpatrick, A. P., Malyala, S. K., & Gibson, I. (2016). *Customised design and development of patient specific 3D printed whole mandible implant*.

Mohammed, M. I., & Gibson, I. (2018). Design of Three-Dimensional, Triply Periodic Unit Cell Scaffold Structures for Additive Manufacturing. *Journal of Mechanical Design, Transactions of the ASME*, *140*(7). https://doi.org/10.1115/1.4040164

Paterson, A. (2013). Digitisation of the splinting process: exploration and evaluation of a Computer Aided Design approach to support Additive Manufacture. *Doctoral Thesis*, 88–100.

Rout, N., Khandual, A., Zhang, Y. F., & Luximon, A. (2010). 3D Foot Scan to Custom Shoe Last. *International Journal of Computer and Communication Technology*, *April*, 110–114. https://doi.org/10.47893/ijcct.2010.1030

Sala, R., Regondi, S., Graziosi, S., & Pugliese, R. (2022). Insights into the printing parameters and characterization of thermoplastic polyurethane soft triply periodic minimal surface and honeycomb lattices for broadening material extrusion applicability. *Additive Manufacturing*, *58*(June), 102976. https://doi.org/10.1016/j.addma.2022.102976

Salles, A. S., & Gyi, D. E. (2013). An evaluation of personalised insoles developed using additive manufacturing. *Journal of Sports Sciences*, *31*(4), 442–450. https://doi.org/10.1080/02640414.2012.736629

Van Netten, J. J., Van Baal, J. G., Liu, C., Van Der Heijden, F., & Bus, S. A. (2013). Infrared Thermal Imaging for Automated Detection of Diabetic Foot Complications. In *Journal of Diabetes Science and Technology* (Vol. 7, Issue 5). www.jdst.org